Hindawi
Journal of Spectroscopy
Volume 2021, Article ID 8811424, 7 pages
https://doi.org/10.1155/2021/8811424

Research Article

Investigation of the Time Behavior of the Second-Order Coherence Function of a Tunable Single-Photon Source

Azadeh Ahmadian and Rasoul Malekfar

Atomic and Molecular Group, Department of Physics, Faculty of Basic Sciences, Tarbiat Modares University, P.O. Box 14115-175, Tehran, Iran

Correspondence should be addressed to Rasoul Malekfar; malekfar@modares.ac.ir

Received 5 September 2020; Accepted 19 May 2021; Published 2 June 2021

Academic Editor: Jau-Wern Chiou

Single-photon sources are critical optical components in quantum communication, in particular, for security applications. One of the essential parameters that define these sources is the magnitude of the second-order coherence function, whose investigation reveals the state of the emitted photon. In this study, we indicate that the second-order coherence function varies over time when using two lasers and preparing coherent population trapping. The calculation is based on solving the master equation to find the density matrix corresponding to the emission dynamics and provide the second-order coherence function. The changes of the second-order coherence function can be estimated and the system behavior regarding photon emission can be predicted by solving the master equation based on the parameters obtained from the experimental results of a nitrogen vacancy (NV) in a diamond. Here we report, for the first time to the best of our knowledge, that the state of the emitted photons persists in the strong interaction of the aforementioned process. As using two lasers is a familiar method for controlling the single-photon source and the stability of the source is an essential point in a quantum network, this study can be considered to develop quantum network components such as memory and on-demand single-photon sources. Also, it suggests a method for tuning photon statistics while controlling the photon states.

1. Introduction

Quantum theory has enabled scientists to study phenomena beyond the classical level and opened new horizons for them. At the beginning of this theory, the existence of separate photons was theoretically suggested by many researchers [1–3], but now it has been shown experimentally [4–7]. To conduct quantum experiments and introduce new technologies, quantum light sources that can emit separate photons, i.e., single-photon sources, have attracted significant research interests [8–12].

Single-photon sources which emit individual photons can send information by each photon, without influencing the information transmitted by the previous photon in the sequence. An optimal single-photon source should deterministically deliver one, and only one, photon at a time, with no trade-off between the source's efficiency and the photon indistinguishability [13].

In a simple model, the detected photons of a single-photon source, which contains just two energy levels and is excited by a pump laser, originate from the transitions between the excited and ground states, as the excited state is populated and cannot absorb another photon. In this case, there is a separation time between two successive emitted single-photons depending on the excited state lifetime. This time separation is the main point for the separation of photons.

Single-photon sources are critical optical components in quantum communications, in particular, for security applications and are employed in quantum communications research both theoretically [14–18] and experimentally [8, 19–21]. In this regard, researchers have studied their

potential applications, for example, in fiber optical windows, along with other technologies, especially those operating at room temperature. Furthermore, researchers have focused on developing on-demand sources as one of the critical components for realizing quantum networks [22–27], and indeed, the introduction of highly controllable sources is of great significance.

There are several methods for controlling the emitted single-photons. One of these methods is coherent population trapping (CPT), which occurs when two resonant optical fields interact with an atom, causing the emission from the excited state to disappear, and there is no emission after lifetime of the excited state. For employing a source in a quantum network, the correlation between the emitted single photons at two successive times needs to be informed; therefore the dynamics of the source states should be studied. If the source is stable at the single-photon level and its regime persists over time, the case would be desirable for the quantum network. So far, various important papers have studied the CPT and time evolution of the related atom states. Also, there are papers describing the preparation of CPT in real systems such as single-photon sources [28, 29]. However, up to now, the stability of the source regime in the emitted photon state has not been studied, which is the primary point of this research. While many researchers have used the CPT phenomena for tuning a single-photon source, we explore its impact on the values of the second-order coherence function, as a function of time.

To this end, we study the time evolution of the excited state of the considered system and the emitting mechanisms of single-photons from the supposed source. We are also motivated to study the correlation of the photons since the CPT condition prepares for a limited time, and after that, the system begins to emit photons [29]. In this respect, the second-order coherence function of the source $g^2(t)$ is investigated, where $g^2(t)$ is the correlation between the intensities of the fields, while t is their time separation. The variations of the second-order coherence function g2 (t) caused by the coherent population trapping (CPT) are examined employing experimental results of a real system. For this purpose, a nitrogen vacancy (NV) in diamond has been chosen as an actual single-photon source. NV in diamond consists of the nearest neighbor pair of a nitrogen atom and a lattice vacancy. It is one of the most significant room-temperature single-photon sources, as it enjoys a unique structure and extraordinary quantum properties for quantum communications, spintronics, quantum information processing, etc. [14, 30–32], and control processes such as CPT and electromagnetically induced transparency processes have been experimentally observed for it [25, 33]. In the next step, using approximation methods, the modifications of $g^2(t)$ function when CPT are prepared have been reported. We show that the intensity profile changes after applying the second laser and preparing the CPT condition. This change affects $g^2(t)$ function, but it is not effective on the regime of the single-photon state.

Therefore, this process can be considered in technology for achieving the desired quantum source in a quantum network. Also, this study can be employed for introducing a method that provides a tunable second-order coherence function and a highly sensitive device with potential applications in quantum communication security.

2. Methods

The second-order coherence function $g^2(t)$ is a function of the time, whose value for $t = 0$ reveals whether the system is a single-photon or not. For $t \neq 0$, assuming a two-level system, i.e., one excited and one ground state, $g^2(t)$ is a function of the spontaneous emission rate. By changing the rate, $g^2(t)$ may be modified. If the Rabi frequency Ω of this system, which is defined as the transition frequency between the ground and excited states, is far smaller than the spontaneous decay rate, γ, the joint probability of detecting two successive photons is [1, 2]

$$g^2(t) = \left[1 - \exp\left(-\frac{\gamma}{2}t\right)\right]^2, \quad \text{for } \Omega \ll \gamma, \tag{1}$$

where $\tau = 1/\gamma$ is the lifetime of the excited state and the first photon is at time $t = 0$ and the other photon is at time $t = \tau$.

Since the aim of this study is to investigate a three-level atom and indicate the changes of $g^2(t)$, an isolated atom including two ground and one excited states,$|1\rangle$, $|2\rangle$, and $|3\rangle$, respectively, is considered. The CPT condition (Figure 1) is prepared and the density of states and related probabilities are calculated.

In the beginning, the atom is in its ground state, after which the pump laser excites the atom. Also, the other laser, which is called the probe or coherent laser and has a frequency close to the pump frequency, is activated, hence satisfying the CPT condition (the formation of the dark state in the excited state).

It can be expected that if the CPT condition is imposed on the system, a reduction of the emission rate should occur within a specific frequency range. It can be expressed using the Einstein coefficients [24]:

$$\gamma(\text{total transition probablity}) = \frac{1}{\tau_3^{\text{eff}}} = A_{32} + A_{31} + \rho(\nu_{31})B_{31} + \rho(\nu_{32})B_{32} + \text{other transition probabilities}, \tag{2}$$

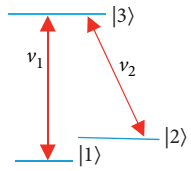

FIGURE 1: Isolated three-level atom in the presence of the pump v_1 and probe v_2 laser interactions.

where $\rho(v_{31})$ and $\rho(v_{32})$ represent energy densities and A_{31} and A_{32} are the spontaneous emission probabilities, while B_{31} and B_{32} are the stimulated emission probabilities between the third and first, as well as third and second levels, respectively.

It seems that in a three-level atomic system, the third atomic energy level is eliminated after the CPT process. It vanishes the coefficients A_{31}, B_{31}, A_{32}, and B_{32}; the effective lifetime of the excited state changes, and equation (1) becomes

$$\frac{1}{\tau_i} = \text{otherstransition probabilities}. \tag{3}$$

The rates of the other transitions are most likely to change. Hence, it is suitable to study the density of states' dynamics for finding the lifetime as well as the second-order coherence function, which are essential parameters.

For the considered system, the Hamiltonian at the initial time, before applying the lasers, is

$$\mathcal{H}_0 = hv_1|1\rangle\langle 1| + hv_2|2\rangle\langle 2| + hv_3|3\rangle\langle 3|. \tag{4}$$

When the lasers are employed, a perturbation appears, where the total Hamiltonian becomes [33]

$$\mathcal{H} = \mathcal{H}_0 + \mathcal{H}_1, \tag{5}$$

$$\mathcal{H}_1 = \frac{h}{2}\left(\Omega_1 e^{-i\phi_1} e^{-iv_1 t}|3\rangle\langle 1| + \Omega_2 e^{-i\phi_2} e^{-iv_2 t}|3\rangle\langle 2|\right) + H.C, \tag{6}$$

where $\Omega_1 e^{-i\phi_1}$ and $\Omega_2 e^{-i\phi_2}$ are the complex Rabi frequencies associated with the coupling of the field modes of frequencies v_1 and v_2 to the atomic transitions $|3\rangle \longrightarrow |1\rangle$ and $|3\rangle \longrightarrow |2\rangle$, respectively.

For the considered system, we solve the density matrix master equation to find the density of the third level in the steady state:

$$\frac{d\rho}{dt} = -i\left[\frac{\mathcal{H}}{\hbar}, \rho\right] + \mathcal{L}(\rho) = 0. \tag{7}$$

The Hamiltonian and decoherence or relaxation terms $\mathcal{L}(\rho)$ are [33]

$$\frac{\mathcal{H}}{h} = \begin{bmatrix} v_1 & 0 & \frac{\Omega_1^*}{2} \\ 0 & v_2 & \frac{\Omega_2^*}{2} \\ \frac{\Omega_1}{2} & \frac{\Omega_2}{2} & v_3 \end{bmatrix}, \tag{8}$$

$$\mathcal{L}(\rho) = \begin{bmatrix} \Gamma_{12}(\rho_{22} - \rho_{11}) + (\Gamma_3)\rho_{33} & -\gamma_{12}\rho_{12} & -\gamma_{13}\rho_{13} \\ -\gamma_{21}\rho_{21} & \Gamma_{12}(\rho_{11} - \rho_{22}) + (\Gamma_3)\rho_{33} & -\gamma_{23}\rho_{23} \\ -\gamma_{31}\rho_{31} & -\gamma_{32}\rho_{32} & -(\Gamma_3)\rho_{33} \end{bmatrix}. \tag{9}$$

After solving the master equation [34], calculating ρ_{33}, and substituting the real parameters of the NV in diamond as a three-level system (see Appendix), the time profile of the density matrix elements can be obtained.

Typically, the intensity is plotted as a function of the detuning frequency from the two photons' resonance process, with the resultant profile displayed in Figure 2.

In this study, we focus on the intensity as a function of the time for the three-level system, i.e., the NV center in diamond and large Rabi frequency. After solving the master equation using the real parameters of the system, we plot the obtained element of the density matrix as a function of time and compare the results. Figure 3 illustrates the changes in the profile before and after applying the second laser, as a function of the time separation. We focus, in particular, on strong interaction between the system and light.

These results inspired us to consider $g^2(t)$ for studying the intensity fluctuations and the relations between two successive photons. Even before performing simulations, we can expect that these differences affect the correlation between intensities $g^2(t)$, as intensity fluctuation changes are suggested from the figure. $g^2(t)$ function has also been plotted (Figure 4). For verifying this statement, the time dependence of the intensity is used and calculated by solving the master equation and substituting the experimental results of the NV in a diamond as a three-level atom [24, 33].

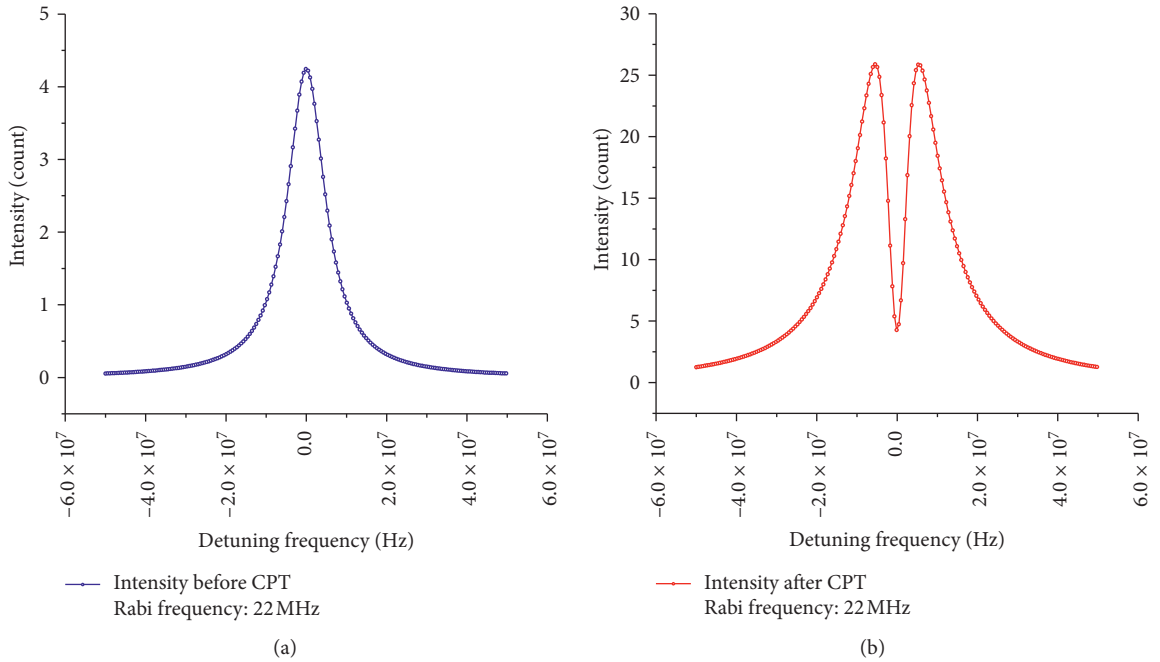

FIGURE 2: Intensity curves (corresponding to ρ_{33}) as a function of the detuning frequency: (a) intensity in the absence of the second laser; (b) intensity in the presence of the second laser.

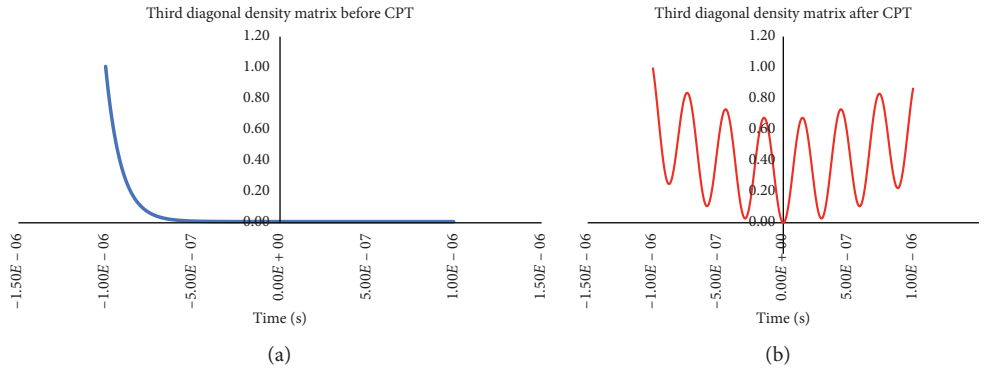

FIGURE 3: Simulation profile of the density matrix element (ρ_{33}) for a NV in a diamond as a function of time when the second laser turns off (a) and turns on (b).

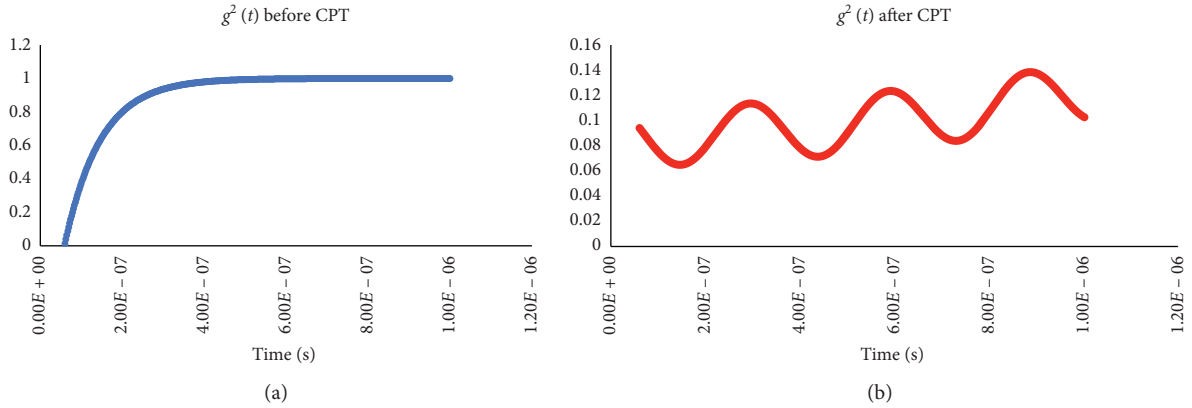

FIGURE 4: Differences between $g^2(t)$ curves: in the absence (a) and in the presence (b) of the second laser.

3. Discussion and Summary

CPT leads to reduced rate of excited-state emission for a range of frequencies. It implies that the electrons prefer to remain in the ground state, i.e., become laser inactive. We employed this variable electron behavior for modifying the effective lifetime of the excited state and emission rate. In other words, CPT provided us with the possibility to alter the rate of emission and, accordingly, the second-order correlation function. As the value of the function is heavily dependent on the system parameters such as the Rabi frequency and frequencies of the lasers, it can be used for investigating the emission behavior of the system.

Another application of this method is to consider it in a photon source, as it can provide a different second-order coherence function. If the value of the second-order coherence function is smaller than 0.5, the source is a single-photon source, while if the value is 1, the states of the emitted photons are coherent (the value measured experimentally for this function for a NV in diamond is approximately 0.07 [3]). In this research, we estimated that $g^2(t)$ changes after CPT, but the emitted photons are still Fock states (after CPT). It implies that the photon wave packets are independent, as before, and the source is a single-photon isolated source. While $g^2(t)$ fluctuations are obvious, its value showed that the source is stable in the single-photon regime. It suggests that the state of the emitted photon is conserved although the second-order coherence function varies after CPT. In many quantum technologies that use the CPT process, such as quantum memories, this effect helps researchers to define the system behavior and avoid the development of undesired events.

In summary, we investigated the second-order coherence function of a three-level single-photon source in the presence of CPT and in the strong interaction. The obtained results were compared with those without CPT. The results suggested that CPT could be used as a method for providing a stable source state, in number or Fock state.

Appendix

For achieving the density matrix elements, the relation [34].

$$\rho_{32}(t) = \frac{i\Omega_2 e^{i\Delta_1 t}}{(\gamma_{32} + 2i\Delta_2)}\rho_{12}, \tag{A.1}$$

is employed, where Ω_2 is the Rabi frequency, which originates from the second laser; γ_{32} is the decay rate between the second and third energy levels; here $\Delta_1 = \omega_{31} - \omega_1$ and $\Delta_2 = \omega_{32} - \omega_1$ are the detunings of the first and second laser frequencies ω_1 and ω_2 from the corresponding atomic transitions.

$$\rho_{12}(t) = -\frac{i\Omega_2 e^{i\Delta_2 t}}{\gamma_{21} + 2i(\Delta_2 - \Delta_1)}\rho_{13}, \tag{A.2}$$

where γ_{12} is the decay rate between the second and first energy levels.

$$\begin{aligned}\rho_{31}(t) &= \frac{i\Omega_1 e^{i\Delta_1 t}}{(\gamma_{31} + 2i\Delta_1)} + \frac{i\Omega_2 e^{i\Delta_2 t}}{(\gamma_{31} + 2i\Delta_1)}\rho_{21} = \frac{i\Omega_1 e^{i\Delta_1 t}}{(\gamma_{31} + 2i\Delta_1)} + \frac{i\Omega_2 e^{i\Delta_2 t}}{(\gamma_{31} + 2i\Delta_1)}\frac{i\Omega_2 e^{-i\Delta_2 t}}{\gamma_{21} - 2i(\Delta_2 - \Delta_1)}\rho_{31} \\ &= \frac{i\Omega_1 e^{i\Delta_1 t}}{(\gamma_{31} + 2i\Delta_1)} + \left[\frac{i\Omega_2 e^{i\Delta_2 t}}{(\gamma_{31} + 2i\Delta_1)}\right]\left[\frac{i\Omega_2 e^{-i\Delta_2 t}}{\gamma_{21} - 2i(\Delta_2 - \Delta_1)}\right]\left[\frac{i\Omega_1 e^{i\Delta_1 t}}{(\gamma_{31} + 2i\Delta_1)}\right],\end{aligned} \tag{A.3}$$

where γ_{31} is the decay rate between the third and first energy levels and Ω_1 represents the Rabi frequency, which is obtained from the first laser.

$$\begin{aligned}\rho_{32}(t) &= \frac{i\Omega_2 e^{i\Delta_1 t}}{(\gamma_{32} + 2i\Delta_2)}\rho_{12} = \frac{i\Omega_2 e^{i\Delta_1 t}}{(\gamma_{32} + 2i\Delta_2)}\left[\frac{-i\Omega_2 e^{i\Delta_2 t}}{\gamma_{21} + 2i(\Delta_2 - \Delta_1)}\rho_{13}\right] \\ \rho_{32}(t) &= \frac{i\Omega_2 e^{i\Delta_1 t}}{(\gamma_{32} + 2i\Delta_2)}\left[\frac{-i\Omega_2 e^{i\Delta_2 t}}{\gamma_{21} + 2i(\Delta_2 - \Delta_1)}\right]\frac{-i\Omega_1 e^{-i\Delta_1 t}}{(\gamma_{31} - 2i\Delta_1)} \\ \rho_{32}(t) &= \left[\frac{\Omega_1 e^{-i\Delta_1 t}}{(\gamma_{31} - 2i\Delta_1)}\right]\left[\frac{\Omega_2 e^{i\Delta_1 t}}{(\gamma_{32} + 2i\Delta_2)}\right]\left[\frac{i\Omega_2 e^{i\Delta_2 t}}{\gamma_{21} + 2i(\Delta_2 - \Delta_1)}\right].\end{aligned} \tag{A.4}$$

For deriving time evolution of the density matrix element $\rho_{33}(t)$, the differential equation which has been solved in detail in reference [29] should be considered.

$$\begin{aligned}\dot{\rho_{33}}(t) = &\frac{i\Omega_2}{2}\left(\rho_{32}e^{i\omega_2 t} - \rho_{23}e^{-i\omega_2 t}\right) + \frac{i\Omega_1}{2}\left(\rho_{31}e^{i\omega_1 t} - \rho_{13}e^{-i\omega_1 t}\right) \\ &- \Gamma_3\rho_{33}.\end{aligned} \tag{A.5}$$

At small vibrations, it can be concluded that

$$\dot{\rho_{33}}(t) = \frac{i\Omega_1}{2}(\rho_{31} - \rho_{13}) + \frac{i\Omega_2}{2}(\rho_{32} - \rho_{23}) - \Gamma_3\rho_{33}. \tag{A.6}$$

By considering

$$\begin{aligned}\rho_{31} &= \rho_{31}^*, \\ \rho_{32} &= \rho_{32}^*,\end{aligned} \tag{A.7}$$

the concluding relation will be

Table 1: The value of parameters in solving the master equation for the coherent population trapping of NV.

$\Omega_1 = \Omega_2$	γ_{21}	γ_{31}	γ_{23}	Δ_1	$\Delta_1 - \Delta_2$
22 THz	3.8 MHz	11.4 MHz	11.4 MHz	470 THz	2.88 GHz

$$\dot{\rho_{33}}(t) = \frac{i\Omega_1}{2} \times 2\mathrm{Im}(\rho_{31}) + \frac{i\Omega_2}{2} \times 2\mathrm{Im}(\rho_{32}) - \Gamma_3\rho_{33} = \Omega_1\rho_{31} + \Omega_2\rho_{32} - \Gamma_3\rho_{33}, \tag{A.8}$$

$$\rho_{33} = \int dt\,(\Omega_1\rho_{31} + \Omega_2\rho_{32} - \Gamma_3\rho_{33}). \tag{A.9}$$

This relation can be simulated by using (A.3), (A.2), and the real value of the experiment [33], as listed in Table 1.

The results of the simulation are presented in Figure 3.

Data Availability

The data used to support the findings of this study are available from the corresponding author upon request.

Conflicts of Interest

The authors declare that they have no conflicts of interest.

References

[1] R. Loudon, *The Quantum Theory of Light*, Oxford, England, 2001.

[2] C. C. Gerry and P. L. Knight, *Introductory Quantum Optics*, Cambridge University Press, Cambridge, UK, 2005.

[3] A. Migdal, S. Polyakov, J. Fan, and J. C. Bienfang, *Single-Photon Generation and Detection*, Elsevier, Amsterdam, Netherlands, 2013.

[4] C. L. Phillips, A. J. Brash, D. P. S. McCutcheon et al., "Photon statistics of filtered resonance fluorescence," *Physical Review Letters*, vol. 125, Article ID 043603, 2020.

[5] C. Jara, T. Rauch, S. Botti et al., "First-principles identification of single photon emitters based on carbon clusters in hexagonal boron nitride," *The Journal of Physical Chemistry A*, vol. 125, no. 6, pp. 1325–1335, 2021.

[6] J. Benedikter, H. Kaupp, T. Hümmer et al., "Cavity-enhanced single-photon source based on the silicon-vacancy center in diamond," *Physical Review Applied*, vol. 7, Article ID 024031, 2017.

[7] Y. P. Korneeva, D. Y. Vodolazov, A. V. Semenov et al., "Optical single-photon detection in micrometer-scale NbN bridges," *Physical Review Applied*, vol. 9, Article ID 064037, 2018.

[8] M. E. Reimer and C. Cher, "The quest for a perfect single-photon source," *Nature Photonics*, vol. 13, no. 11, pp. 734–736, 2019.

[9] F. Ripka, H. Kübler, R. Löw, and T. Pfau, "A room-temperature single-photon source based on strongly interacting Rydberg atoms," *Science*, vol. 362, no. 6413, pp. 446–449, 2018.

[10] J. Wang, Y. Zhou, Z. Wang et al., "Bright room temperature single photon source at telecom range in cubic silicon carbide," *Nat Communications*, vol. 9, Article ID 4106, 2018.

[11] R. S. Daveau, K. C. Balram, T. Pregnolato et al., "Efficient fiber-coupled single-photon source based on quantum dots in a photonic-crystal waveguide," *Optica*, vol. 4, no. 2, pp. 178–184, 2017.

[12] C.-M. Lee, M. A. Buyukkaya, S. Aghaeimeibodi, A. Karasahin, C. J. K. Richardson, and E. Waks, "A fiber-integrated nanobeam single photon source emitting at telecom wavelengths," *Applied Physics Letters*, vol. 114, no. 17, Article ID 171101, 2019.

[13] H. Wang, Y.-M. He, T.-H. Chung et al., "Towards optimal single-photon sources from polarized microcavities," *Nature Photonics*, vol. 13, no. 11, pp. 770–775, 2019.

[14] B. Scharfenberger, H. Kosaka, W. J. Munro, and K. Nemoto, "Absorption-based quantum communication with NV centres," *New Journal of Physics*, vol. 17, no. 10, Article ID 103012, 2015.

[15] R. Qi, Z. Sun, Z. Lin et al., "Implementation and security analysis of practical quantum secure direct communication," *Light: Science & Application*, vol. 8, p. 22, 2019.

[16] T. Li and GL. Long, "Quantum secure direct communication based on single-photon Bell-state measurement," *New Journal of Physics*, vol. 22, 2020.

[17] W. Li, L. Wang, and S. Zhao, "Phase matching quantum key distribution based on single-photon entanglement," *Scientific Reports*, vol. 9, 15466 pages, 2019.

[18] D. Jiang, Y. Chen, X. Gu, L. Xie, and L. Chen, "Deterministic secure quantum communication using a single d-level system," *Scientific Reports*, vol. 7, Article ID 44934, 2017.

[19] S. Thomas and P. Senellart, "The race for the ideal single-photon source is on," *Nature Nanotechnology*, vol. 16, no. 4, 368 pages, 2021.

[20] N. Tomm, A. Javadi, N. O. Antoniadis et al., "A bright and fast source of coherent single photons," *Nature Nanotechnology*, vol. 16, 2021.

[21] C. Cao, YH. Han, X. Yi et al., "Implementation of a single-photon fully quantum router with cavity QED and linear optics," *Optical and Quantum Electronics*, vol. 53, p. 32, 2021.

[22] P. Farrera, G. Heinz, B. Albercht et al., "Generation of single photons with highly tunable wave shape from a cold atomic ensemble," *Nature Communications*, vol. 7, Article ID 13556, 2016.

[23] J. Gulla and J. Skaar, "Approaching single-photon pulses," *Physical Review Letters*, vol. 126, Article ID 073601, 2021.

[24] N. Mizuochi, T. Makino, H. Kato et al., "Electrically driven single-photon source at room temperature in diamond," *Nature Photonics*, vol. 6, no. 5, pp. 299–303, 2012.

[25] V. M. Acosta, K. Jensen, C. Santori, D. Budker, and R. G. Beausoleil, "Electromagnetically-induced transparency in a diamond spin ensemble enables all-optical electromagnetic field sensing," *Physical Review Letters*, vol. 110, Article ID 213605, 2013.

[26] Y. Hu, S. He, Y. Zhang, H. Yuan, WM. Liu, and CH. Yan, "Controllable photon extraction based on a single-photon Raman interaction," *Journal of Physics B*, vol. 54, no. 4, 2021.

[27] A. Ahmadian and R. Malekfar, "Wave packet shaping for a single-photon source," *Journal of the Optical Society of America B*, vol. 38, no. 3, 2021.

[28] A. Donarini, M. Niklas, M. Schafberger, N. Paradisco, C. Strunk, and M. Grifoni, "Coherent population trapping by dark state formation in a carbon nanotube quantum dot," *Nature Communications*, vol. 10, p. 381, 2019.

[29] P. Jamonneau, G. Hétet, A. Dréau, J. F. Roch, and V. Jacques, "Coherent population trapping of a single nuclear spin under ambient conditions," *Physical Review Letters*, vol. 116, Article ID 043603, 2016.

[30] A. Bhaumik, R. Sachan, and J. Narayan, "Tunable charge states of nitrogen-vacancy centers in diamond for ultrafast quantum devices," *Carbon*, vol. 142, pp. 662–672, 2019.

[31] E. Bourgeois, A. Jarmola, P. Siyushev et al., "Photoelectric detection of electron spin resonance of nitrogen-vacancy centres in diamond," *Nature Communicationsn*, vol. 6, 8577 pages, 2015.

[32] M. W. Doherty, N. B. Manson, P. Delaney, F. Jelezko, J. Wrachtrup, and L. C. L. Hollenberg, "The nitrogen-vacancy colour centre in diamond," *Physics Reports*, vol. 528, no. 1, pp. 1–45, 2015.

[33] C. Santori, D. Fattal, S. M. Spillane et al., "Coherent population trapping in diamond N-V centers at zero magnetic field," *Optics Express*, vol. 14, no. 17, pp. 7986–7994, 2006.

[34] G. T. Purves, *Absorption and Dispersion in Atomic Vapours: Applications to Interferometry*, Ph.D. Thesis, University of Durham, Durham, England, 2006.